Journal of Cell Science 112, 4051-4065 (1999)
Printed in Great Britain © The Company of Biologists Limited 1999
JCS0849

Epidermal tendon cells require *Broad Complex* function for correct attachment of the indirect flight muscles in *Drosophila melanogaster*

David J. Sandstrom[1,*] and Linda L. Restifo[1,2,‡]

[1]ARL Division of Neurobiology and [2]Interdisciplinary Program in Genetics, University of Arizona, Tucson, AZ 85721-0077, USA
*Present address: Department of Molecular and Cellular Biology, University of Arizona, Tucson, AZ 85721-0106, USA
‡Author for correspondence (e-mail: llr@neurobio.arizona.edu)

Accepted 14 September; published on WWW 3 November 1999

SUMMARY

***Drosophila Broad Complex*, a primary response gene in the ecdysone cascade, encodes a family of zinc-finger transcription factors essential for metamorphosis. *Broad Complex* mutations of the *rbp* complementation group disrupt attachment of the dorsoventral indirect flight muscles during pupal development. We previously demonstrated that isoform BRC-Z1 mediates the muscle attachment function of *rbp*$^+$ and is expressed in both developing muscle fibers and their epidermal attachment sites. We now report two complementary studies to determine the cellular site and mode of action of *rbp*$^+$ during maturation of the myotendinous junctions of dorsoventral indirect flight muscles. First, genetic mosaics, produced using the *paternal loss* method, revealed that the muscle attachment phenotype is determined primarily by the genotype of the dorsal epidermis, with the muscle fiber and the ventral epidermis exerting little or no influence. When the dorsal epidermis was mutant, the vast majority of muscles detached or chose ectopic attachment sites, regardless of the muscle genotype. Conversely, wild-type dorsal epidermis could support attachment of mutant muscles. Second, ultrastructural analysis corroborated and extended these results, revealing defective and delayed differentiation of *rbp* mutant epidermal tendon cells in the dorsal attachment sites. Tendon cell processes, the stress-bearing links between the epidermis and muscle, were reduced in number and showed delayed appearance of microtubule bundles. In contrast, mutant muscle and ventral epidermis resembled the wild type. In conclusion, BRC-Z1 acts in the dorsal epidermis to ensure differentiation of the myotendinous junction. By analogy with the cell-cell interaction essential for embryonic muscle attachment, we propose that BRC-Z1 regulates one or more components of the epidermal response to a signal from the developing muscle.**

Key words: Metamorphosis, Ecdysone cascade, Genetic mosaic, Myotendinous junction

INTRODUCTION

Normal motor function requires that muscles form stable attachments at correct skeletal locations. Development and maintenance of these attachments are essential for muscle integrity in both immature and adult animals (Newman and Wright, 1981; Margolis and Baker, 1983; Gollvik et al., 1988; Kardon, 1998). While little is known regarding the mechanism of muscle attachment during vertebrate development, genetic studies in the fruitfly *Drosophila melanogaster* are beginning to reveal its cellular and molecular basis.

Insect muscles are attached to the exoskeleton (cuticle) via epidermal tendon cells (reviewed by Smith, 1982). Tendon cells differentiate at epidermal muscle attachments (EMAs), specific locations that express a number of molecular markers (Bogaert et al., 1987; Buttgereit et al., 1991; Volk and VijayRaghavan, 1994; Callahan et al., 1996; Fernandes et al., 1996; Goubeaud et al., 1996; Becker et al., 1997; Yarnitsky et al., 1997). Forces exerted by the muscles are transmitted to the cuticle through a series of muscle and tendon cell specializations (Auber, 1963; Lai-Fook, 1963; Caveney, 1969; Prokop et al., 1998). At the myotendinous junction (MTJ), myofilaments are linked to the muscle membrane by modified terminal Z bands. The membrane of the muscle cell and the basal membrane of the tendon cell interdigitate extensively, with each secured by specialized junctions to the intervening extracellular matrix. Force is transmitted from the basal surface of the tendon cell to its apical (cuticular) surface via bundles of microtubules. During *Drosophila* embryogenesis, differentiation of MTJs requires a molecular conversation between muscle and tendon cells, interruption of which prevents effective muscle attachment (Callahan et al., 1996; Becker et al., 1997; Vorbrüggen and Jäckle, 1997; Yarnitsky et al., 1997; Strumpf and Volk, 1998).

During metamorphosis, the steroid hormone 20-hydroxyecdysone (20E) controls the replacement of larval epidermis and musculature by new adult structures (Bate, 1993; Fristrom and Fristrom, 1993). This developmental transition provides another opportunity to study genetic control and cellular mechanisms of muscle attachment. We have shown

(Sandstrom et al., 1997) that correct and stable attachment of the large thoracic muscles of adult *Drosophila* requires a subset of Broad Complex (BRC) transcription factors (DiBello et al., 1991; von Kalm et al., 1994), products of a 20E-inducible gene (Chao and Guild, 1986; Huet et al., 1993; Karim et al., 1993; Bayer et al., 1996a; Restifo and Hauglum, 1998) involved in many aspects of metamorphosis (Kiss et al., 1988; Restifo and White, 1991, 1992; reviewed by Bayer et al., 1996b). Here we report genetic and ultrastructural studies that reveal BRC-dependent sites and events during thoracic muscle attachment.

BRC mutants of the *rbp* (*reduced bristles on palps)* complementation group have distinctive defects involving the most prominent thoracic muscles of adult *Drosophila*, the indirect flight muscles (IFM) and tergotrochanteral, or jump, muscle (TTM) (Restifo and White, 1992). The IFM consist of dorsal longitudinal (DLM) and dorsoventral IFM (DVM), which are morphologically and biochemically specialized to produce the high contraction frequencies required for dipteran flight; TTM is a tubular muscle, resembling the other somatic muscles (reviewed by Bernstein et al., 1993; Dickinson and Tu, 1997). *rbp* mutants have few intact DVM fibers, and these, along with the DLM and TTM, are often attached to incorrect EMAs (Fig. 1; Sandstrom et al., 1997).

IFM and TTM develop from myoblasts (called adepithelial cells because they are associated with the imaginal disc epithelium), which proliferate during larval and early pupal life (reviewed by Bate, 1993; Fernandes et al., 1991). Early during metamorphosis, the myoblasts migrate, fuse with one another to form muscle primordia, and align between their respective EMAs (Shatoury, 1956; Costello and Wyman, 1986; Fernandes et al., 1991; Reedy and Beall, 1993a). Subsequent maturation of the IFM includes stereotyped morphological changes that yield the differentiated muscles and elaborate MTJs of the adult fly (Auber, 1963; Reedy and Beall, 1993a,b).

Our developmental analysis demonstrated that rbp^+ (i.e. wild type) function is required for the IFM and TTM to establish and maintain attachment to epidermal tendon cells at correct EMA sites (Sandstrom et al., 1997). In *rbp* mutants, thoracic muscle primordia make contact with EMAs during early pupal life. However, most incipient attachments of DVM with dorsal thoracic EMAs are unable to withstand the muscle shortening that occurs several hours later, resulting in muscle detachment, generally followed by complete degeneration. In addition, significant numbers of mutant muscles form junctions with inappropriate EMAs, e.g. DLM attaching to DVM sites. These defects can be completely rescued by expressing specific BRC isoforms (BRC-Z1 or -Z4, but not -Z2 or -Z3) from inducible transgenes at the beginning of pupal development.

These data suggest that *rbp* mutations disrupt the interaction between developing epidermal tendon cells and muscles. BRC-Z1, the primary mediator of rbp^+ function, is expressed in both thoracic epidermis and muscles of wild-type pupae (Sandstrom et al., 1997). The rescuing transgenes are heat-shock-driven (Bayer et al., 1997) and, therefore, expressed in all tissues (Pauli et al., 1992). Hence, we did not know which side of the cell-cell interaction fails in the mutants. In order to determine where rbp^+ function is required for normal muscle attachment, we analyzed mosaic animals whose thoracic muscles and epidermis were of different genotypes. We also compared developing MTJs of mutant and wild type and identifed subcellular defects resulting from reduced rbp^+ function. Data from these two complementary approaches point to the dorsal EMA as the essential site of rbp^+ action in controlling muscle attachment.

MATERIALS AND METHODS

Strains and stocks

Cultures were reared at 25°C on standard corn flour/yeast/agar medium (Elgin and Miller, 1978). Canton-S was the wild-type strain used. *rbp* (*reduced bristles on palps*) mutant strains were as described previously (Restifo and White, 1991; Sandstrom et al., 1997). *pal* was a generous gift from Jeff Hall (Brandeis University). *Mhc-lacZ* flies, bearing an X-linked P-element transgene in which the β-galactosidase (βgal) coding region was fused to the *Myosin heavy chain* promoter (Hess et al., 1989), were kindly provided by Sandy Bernstein (San Diego State University). *y w* sn^3 was obtained from the *Drosophila* Stock Center at Bowling Green, KY. The TTM-specific enhancer-trap line *BTJ 629* (Anand et al., 1990) was generously provided by Anne Schneiderman (Cornell University). Marker mutations are as described by Lindsley and Zimm (1992).

Generation and analysis of mosaics

Mosaics were generated using the *paternal loss* (*pal*) mutation (Baker, 1975), with modifications of the protocol of Ewer et al. (1992). Progeny of *pal* males lose one or more paternal chromosomes during one of the earliest nuclear divisions, resulting in large hemizygous clones which encompass, on average, slightly less than half of the body (Baker, 1975). Although any paternal chromosome can be lost, only those clones hemizygous for the X and fourth chromosome are recovered, because loss of a second or third chromosome is cell-autonomous lethal. In all crosses, a single *Mhc-lacZ/Y; pal* male was mated with 3-4 females of the appropriate genotype (see below), and transferred every 2-4 days. The frequency of mosaic progeny varied among parental males, ranging from 0% to 7.5%.

To determine the site of rbp^+ action in muscle attachment, *Mhc-lacZ/Y; pal* males were crossed with *y* rbp^5 w^a sn^3/*Binsn; +* females. In the progeny, diplo-X tissues, carrying both maternal and paternal X chromosomes (*y* rbp^5 w^a sn^3/*Mhc-lacZ)*, exhibit wild-type eye color, cuticular pigmentation and bristle morphology, and βgal expression in skeletal muscle. Late pupae carrying the balancer chromosome (*Binsn/Y* or *Mhc-lacZ/Binsn*) were distinguished by the eye-shape phenotype conferred by the dominant marker *Bar*. Haplo-X tissues (carrying only the maternal X chromosome, *y* rbp^5 w^a sn^3) reveal the recessive markers in the eye and epidermis, and do not express βgal in muscle. Because epidermal tendon cells secrete overlying epidermis as well as acting as muscle attachments (Smith, 1982), the cuticular phenotype is a direct reflection of the tendon cell genotype. In addition, because they are male, haplo-X clones in sexually dimorphic regions produce male structures such as sex combs and male genitalia. Therefore, mutant (*y* rbp^5 w^a sn^3/*0*) clones in *y* rbp^5 w^a sn^3/*Mhc-lacZ; pal*/+ pharate adults were identified on the basis of *y* cuticle and *sn* bristles, w^a eye color, and/or male structures. These 'experimental' mosaics were collected and the locations of mutant clones recorded. To determine the genotypes and phenotypes of the IFM and TTM, thoraces of all mosaics, regardless of the presence of thoracic clones, were histochemically stained to visualize βgal activity and then sectioned for morphological analysis (see below). Of 3959 *y* rbp^5 w^a sn^3/*Mhc-lacZ; pal*/+ pharate adult progeny examined, 17 experimental mosaics were identified, and 16 were analyzed.

To reveal any effects of cuticular markers, βgal expression, or mosaicism per se, *Mhc-lacZ/Y; pal* males were crossed with *y w* sn^3 females. Of 7674 *y w* sn^3/*Mhc-lacZ; pal*/+ progeny, 23 'control' mosaics were identified and scored as above, with the exception that

some were collected after emergence, and hemizygous eye clones were *w* rather than w^a. Of these, eight mosaics were collected as pharate adults and processed for thoracic muscle analysis. The remaining 15 mosaics had already eclosed and were not included in this study, because the corresponding experimental mosaics were analyzed as pharate adults, and also because the muscles of emerged adults stained poorly with our methods. Additional controls included non-mosaic siblings of the mosaic animals (*y* rbp^5 w^a sn^3*/Mhc-lacZ; pal/+*, *y* rbp^5 w^a sn^3*/Y; pal/+*, *y w* sn^3*/Mhc-lacZ; pal/+*), and progeny from a cross between *Mhc-lacZ/Y; +* and *y w* sn^3 (*y w* sn^3*/Mhc-lacZ; +*).

DVM data from mosaic animals were analyzed by Chi-square testing (Sokal and Rohlf, 1993). For comparisons with wild type, expected proportions of normal and abnormal muscles were based on *y w* sn^3 control mosaics. For comparison with *rbp* mutants, expected proportions were based on the non-mosaic *y* rbp^5 w^a sn^3*/Y; pal/+* siblings of the experimental mosaics.

Staging

Progeny from all mosaic-producing crosses were transferred to humid chambers within 24 hours after pupariation and aged at 25°C to the late pharate adult stage (stage P15; Bainbridge and Bownes, 1981). This prevented the dessication and premature death of *rbp* mutant pupae that typically occurs in standard culture vials. For electron microscopy studies, animals were collected as white prepupae, aged in humid chambers, and staged on the basis of time after head eversion (which occurs approximately 12 hours after pupariation) and other morphological criteria (Bainbridge and Bownes, 1981), as described previously (Sandstrom et al., 1997). This procedure maximized developmental synchrony between wild-type and mutant pupae.

Histological techniques

βgal activity was visualized in thoraces of pharate adults using a modification of standard histochemical methods (Ashburner, 1989; Liu and Restifo, 1998). Note that all samples used in the mosaic analysis underwent the same processing, regardless of whether they carried the *Mhc-lacZ* transgene. After removal of the head, wings, legs, and abdomen, the thorax was fixed in 1% glutaraldehyde (Ted Pella) for 6-24 hours (12 hours was optimal) at 4°C, followed by 3 hours at room temperature. After 3 washes of 30 minutes each in PBS, the thorax was incubated in X-gal (Sigma) reaction buffer at 37°C for 9-36 hours (12 hours was best). Stained tissue was postfixed in FAAG (an aqueous solution of 4% formaldehyde, 85% ethyl alchohol, 5% acetic acid, and 1% glutaraldehyde; Campos et al., 1985) for 3 hours at room temperature, embedded in paraffin as described previously (Restifo and White, 1991), and cut at 10 μm on a rotary microtome. Endogenous βgal activity in thoraces of Canton-S pharate adults processed in this manner was limited to non-muscle tissue such as tracheae, small cells presumed to be hemocytes, and clusters of large, intensely-staining cells near the primary tracheal trunks in the anterior thorax (e.g. Fig. 3C). To assess the extent of diffusion of X-gal reaction product during processing, thoraces from an enhancer trap line with specific expression in the TTM (*BTJ 629*; Anand et al., 1990) were stained and sectioned; no appreciable diffusion of stain between muscles was observed.

Serial sections through the entire thorax were examined to ascertain the genotypes and phenotypes of DVM, DLM, and TTM fibers. In some cases, staining of βgal-expressing muscle was weaker in central regions of the thorax, but DLM genotypes could be assigned unambiguously when muscles were examined at several sites. The genotypes of detached muscle remnants could be determined because *Mhc*-directed βgal expression begins by 12-14 hours after head eversion (Fernandes et al., 1991), when *rbp* mutant muscles appear relatively healthy, and the enzyme either remained active until the pharate adult stage, or the detached muscles continued to express βgal. In the vast majority of cases, the identities of DVM I, II, and III could be established on the basis of their ventral attachment sites because *rbp* mutations do not cause ectopic ventral attachments (Sandstrom et al., 1997). Rarely, ventral detachment of a DVM required that the dorsal attachment site be used to assign its identity. For the preparation of Figures, digital images of specimens were obtained with a Sony camera (model DKC-500) on a Leitz Diaplan microscope, and were converted to grayscale and labeled using Corel PhotoPaint and Corel Draw v.8.0.

Electron microscopy

Early-stage *Drosophila* pupae are difficult to process for electron microscopy because of their small size, delicacy, and high fat content. For this reason, tissue fixation and processing were performed in the presence of microwaves, which provided superior ultrastructural preservation and in a considerably shorter time than achieved with conventional methods. Fixation, en bloc staining, dehydration and infiltration were carried out in a 900-Watt microwave oven (Pelco 3450, Ted Pella Inc.), based on previously-described methods (reviewed by Kok and Boon, 1992; Login and Dvorak, 1994) and specific suggestions from the manufacturer. For fixation and en bloc staining, the temperature control was set to 37°C and the temperature probe was placed in a large beaker of water inside the oven. Samples were cooled on ice for 5-10 minutes between treatments. Under these conditions, each microwave bout increased the sample temperature (measured directly with the probe before and after each exposure) by 10-15°C.

Pupae were removed from puparia under ice-cold PBS, holes were cut in the wings and posterior abdomen, and proboscises were removed to facilitate entry of fixative. Individuals were placed in 0.6 ml fixative containing 3% glutaraldehyde (Ted Pella) and 0.2% tannic acid (EM Science) in 0.1 M cacodylate buffer, 5 mM $MgCl_2$, pH 7.2 (modified from Reedy and Reedy, 1985; Reedy and Beall, 1993a,b), and subjected to microwaves for two bouts of 40 seconds each. Pupae were then embedded in 7% low-melting-point agarose (VWR Scientific) and their heads and abdomens were removed with a Vibratome (Technical Products International, St Louis, MO). Thoraces were placed in fresh fixative, and subjected to microwaves for two additional 40-second bouts, and then washed twice with 0.1 M cacodylate, 10 mM $MgCl_2$.

After glutaraldehyde/tannic acid fixation, the agarose was removed, and pupae were postfixed in 2% osmium tetroxide (Ted Pella) in 0.1 M cacodylate, 5 mM $MgCl_2$ for three bouts of microwaving, each lasting 40 seconds, separated by 10 minutes of cooling on ice. They were then washed once each with cacodylate/$MgCl_2$ buffer and distilled H_2O. En bloc staining with 1% uranyl acetate (Fisher Scientific) in distilled H_2O was performed in the microwave oven using a single 40-second exposure, followed by 10 minutes on ice.

Dehydration in a graded alcohol series was performed using 40-second microwave exposures, with the temperature probe placed directly in the alcohol, and no cooling steps between exposures. Samples were infiltrated with low-viscosity Spurr's resin (Ted Pella) by placing them in a 1:1 mix of resin and ethanol, microwaving for 15 minutes, and then placing them in two changes of fresh resin and microwaving for 10 minutes each, maintaining the temperature at 35°C with the probe directly in the resin. Samples were transferred to fresh resin in silicone molds and polymerized overnight at 60°C in a conventional oven.

All thoraces were sectioned in the frontal plane. Semithin (0.5-1.0 μm) sections were stained with 1% toluidine blue O in 1% borax and used for orientation. Thin sections (60-70 nm) were obtained using a diamond knife, mounted on Formvar-coated slot grids (Ted Pella) and stained with saturated aqueous uranyl acetate, followed by 2% lead citrate (Reynolds, 1963). Thin sections were viewed with JEOL JEM 1200EX or Phillips CM12 transmission electron microscopes. Interpretations are based on at least four animals per stage and genotype. Photomicrographs were printed from negatives, scanned at 300-600 dpi using Deskscan II software (Hewlett-Packard), and

montages were assembled and labeled using Corel PhotoPaint and Corel Draw v.8.0.

RESULTS

rbp$^+$ function is required in the dorsal epidermis for normal muscle attachment

BRC-Z1 is expressed in the dorsal and ventral EMAs, and in the IFM and TTM themselves during a critical developmental period (Sandstrom et al., 1997), and therefore *rbp*$^+$ may act at any or all of these sites to establish and maintain stable muscle attachments at the correct locations. To determine which of these requires *rbp*$^+$ function, we used the *paternal loss* (*pal*) mutation (Baker, 1975) to produce genetic mosaics with both *rbp* mutant and wild-type tissues. A similar strategy was used to reveal the site of *shibire*$^+$ action in IFM development (Hummon and Costello, 1993). Because *pal* induces chromosome loss very early in development, we were able to recover mosaic animals in which thoracic muscles and their EMAs had different genotypes. *rbp* mutant epidermal clones were identified on the basis of the recessive markers *yellow* and *singed* on the maternally-inherited X chromosome. Wild-type muscle was identified on the basis of βgal expression, provided by a muscle-specific *lacZ* transgene on the paternal X chromosome; mutant muscles lacked the *Mhc-lacZ* transgene and therefore did not express βgal. Muscle remnants bearing the *Mhc-lacZ* transgene continued to display βgal activity at advanced stages of degeneration (see below).

rbp^5 was selected for the mosaic analysis, because it is the strongest extant *rbp* allele and its DVM phenotype is fully penetrant (Sandstrom et al., 1997). For the characterization of the DVM phenotype, the units of analysis were whole muscles (e.g. DVM I, which consists of three fibers), rather than individuals fibers, thus avoiding potential confusion resulting from fasciculation defects.

Each DVM was placed in one of the following phenotypic categories:
Normal: all fibers attached to correct EMAs;
Ectopically Attached: one or more fibers spanning the full height of the thorax, but attached to an incorrect dorsal EMA;
Detached Dorsally: one or more fibers detached from their dorsal EMA, leaving remnants in the ventral thorax;
Detached Ventrally: one or more fibers detached from their ventral EMA and recoiled dorsally;
Absent: all fibers missing, leaving no remnants.

The baseline *rbp* phenotype, assessed in *y rbp*^{5} *w*^{a} *sn*^{3}*/Y; pal/+* siblings of the experimental mosaics, did not differ from that reported previously (Sandstrom et al., 1997) with 92% (55/60) of DVM showing defects (Fig. 2A). The abnormalities fell into the same categories, except that one fiber (2%) had detached from its ventral EMA, leaving a remnant in the dorsal thorax. This ventral detachment phenotype had not been observed previously, presumably because it is so rare.

All DVM were normal in several non-mosaic, wild-type control groups examined (Fig. 2A): *y w sn*^{3}*/Mhc-lacZ; pal/+*, *y w sn*^{3}*/Mhc-lacZ; +*, and *y rbp*^{5} *w*^{a} *sn*^{3}*/Mhc-lacZ; pal/+*. Thus, neither the recessive markers nor the transgene affected DVM attachment.

Among the mosaic animals, both experimental (*y rbp*^{5} *w*^{a} *sn3/0; n*=16) and control (*y w sn*^{3}*/0*; n=8) haplo-X epidermal clones were generally contiguous and large, with a wide range of sizes as described previously (Baker, 1975). In one individual, the only detectable mutant epidermis was a tiny patch on the dorsal notum, whereas, in another, the entire thorax, abdomen and most of the head were mutant. Because each muscle fiber is a syncitium and the βgal marker is cytoplasmic, we would not have been able to identify DVM containing both mutant and wild-type nuclei. However, in *pal*-induced mosaics, a clonal boundary would only very rarely cross a single DVM. Moreover, based on the βgal marker, all IFM on a given side had the same genotype (e.g. Fig. 3A). In contrast, the genotypes of ipsilateral IFM and non-IFM (e.g. leg and direct flight muscles) sometimes differed (Fig. 3A), consistent with previous studies demonstrating that the IFM and a subset of non-IFM arise from distinct primordia (Lawrence, 1982).

DVM phenotypes in mosaics

Of 96 possible DVM in experimental mosaics (16 animals with three DVM per side), the genotypes of 70 muscles and of their attachment sites were unambiguous. Of the remaining 26 DVM, 17 had degenerated completely, leaving no remnants. However, because all IFM on a given side had the same genotype, those of the missing muscles were inferred from those of ipsilateral DLM and surviving DVM. Hence, the genotypes of muscles scored as ‘absent’ were not determined directly. Nine DVM were not included in the quantitative

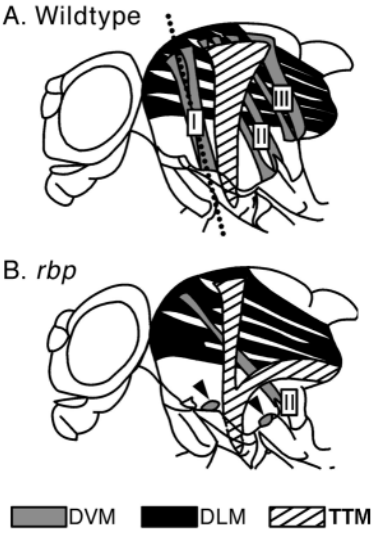

Fig. 1. Schematic representations of wild-type and *rbp* mutant thoracic muscles (adapted from Williams and Williams, 1943). (A) Canton-S. The indirect flight muscles (IFM) consist of the dorsal longitudinal (DLM, black) and dorsoventral (DVM, gray) indirect flight muscles. DLM contains six fibers per side, while DVM is composed of 7 fibers per side, divided into three muscles, DVM I (I, three fibers), DVM II (II, two fibers) and DVM III (III, two fibers). The tergotrochanteral muscle (TTM, hatched) comprises approximately 30 fibers running dorsoventrally. The dotted line indicates the approximate plane of section in Figs 3-9. (B) *rbp*^{1} mutant, typical features. Many DVM fibers have detached from the dorsal thorax, leaving either remnants (e.g. DVM I and II, arrowheads), or no trace (e.g. DVM III), while other muscles (e.g. the remaining DVM II fiber and the posterior TTM fibers) are attached to incorrect epidermal muscle attachment sites (EMAs).

analysis because a clonal boundary occurred at or very near to one of their EMAs; these were nonetheless instructive (see below).

Of the 39 DVM in experimental mosaics in which the muscle and both of its EMAs were genotypically wild type, 38 (97%) were phenotypically normal (Fig. 2A). Surprisingly, one DVM (3%) had detached dorsally, perhaps due to infrequent, non-specific effects of *pal* (see below). All three DVM for which the muscles and both attachment sites were *rbp* showed a mutant phenotype; two DVM were missing and the third had an ectopic dorsal attachment site (Fig. 2A). These observations are consistent with the hypothesis that the phenotype of the

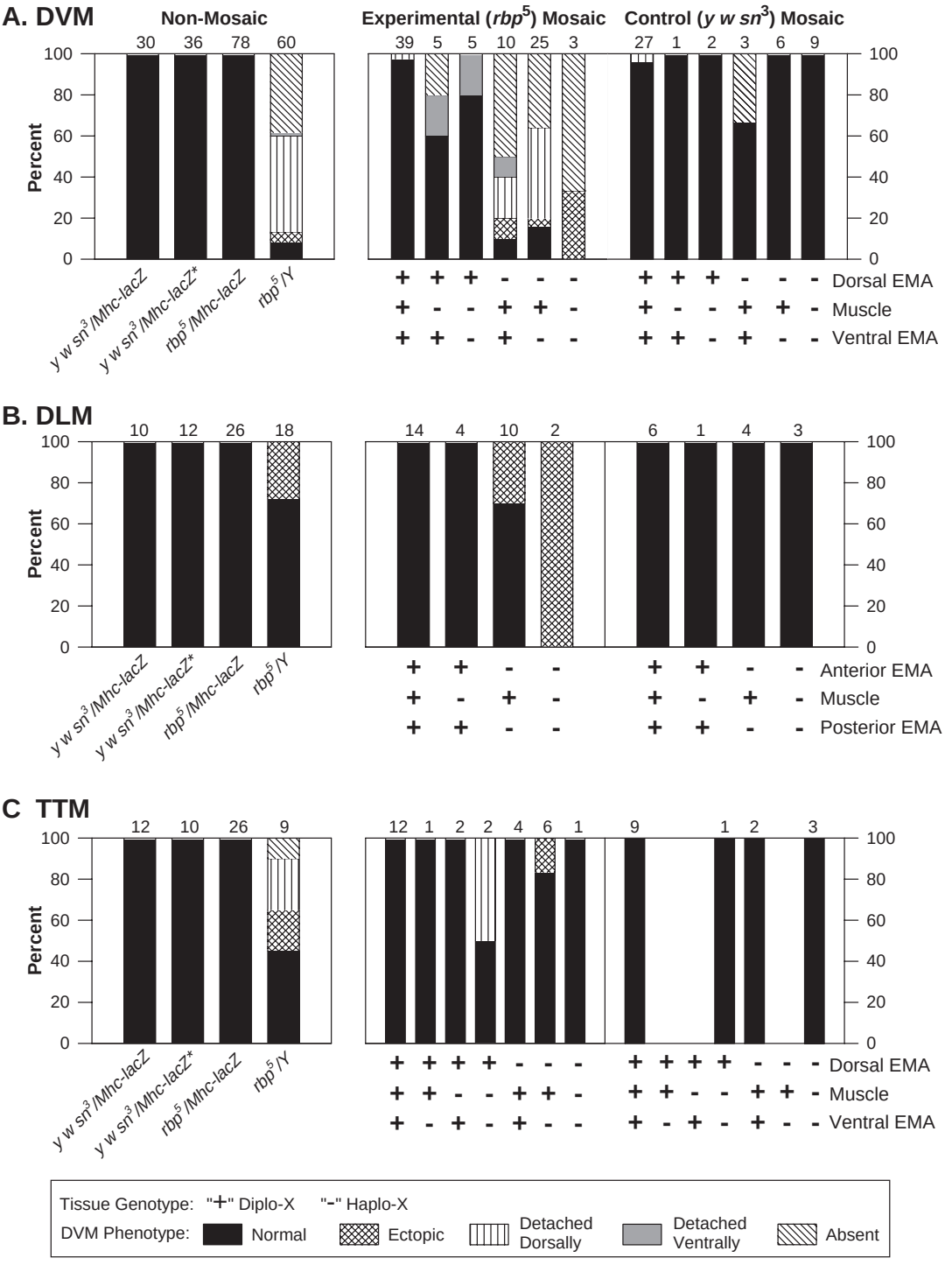

Fig. 2. Effects of tissue genotype on muscle phenotype. The stack bars indicate the percentage of muscles falling into the phenotypic classes (see legend) described in the text for DVM (A), DLM (B), and TTM (C). The leftmost plots show data from non-mosaic controls, the center plots show results from *y rbp*^{5} *w*^{a} *sn*^{3}*/Mhc-lacZ; pal/+* ('experimental') mosaics, and the rightmost plots show the results from *y w sn*^{3}*/Mhc-lacZ; pal/+* ('control') mosaics. For the non-mosaics, *y w sn*^{3}*/Mhc-lacZ* denotes *y w sn*^{3}*/Mhc-lacZ; pal/+*, *rbp*^{5}*/Mhc-lacZ* denotes *y rbp*^{5} *w*^{a} *sn*^{3}*/Mhc-lacZ; pal/+*, and *rbp*^{5}*/Y* denotes *y rbp*^{5} *w*^{a} *sn*^{3}*/Y; pal/+*, all siblings of the mosaics. *y w sn*^{3}*/Mhc-lacZ** denotes *y w sn*^{3}*/Mhc-lacZ; +* from a separate cross. For mosaics, the genotypes of muscles and EMAs are given below each bar, with '+' indicating diplo-*X* and '-' indicating haplo-*X*. Numbers above bars indicate the numbers of muscles scored. (A) DVM. DVM were normal in wild-type non-mosaic controls, but virtually all DVM of *rbp*^{5}*/Y* mutants were abnormal. Among the *rbp*^{5} mosaics, DVM with mutant dorsal EMAs had the most severe phenotypes, regardless of the genotype of the muscle or ventral EMA. *y w sn*^{3} mosaics had a low incidence of DVM defects, the presence of which was not correlated with muscle or epidermal genotype. (B) DLM. Wild-type controls showed no DLM defects, while *rbp*^{5}*/Y* caused some ectopically attached fibers. In experimental mosaics, DLM only showed ectopic attachment when the EMAs were mutant. The DLM of control mosaics had normal attachments. (C) TTM. Among the non-mosaic controls, only *rbp*^{5}*/Y* animals had defective TTM. In experimental mosaics, only two TTM showed defects, and both of these had mutant ventral EMAs. TTM of control mosaics were phenotypically normal.

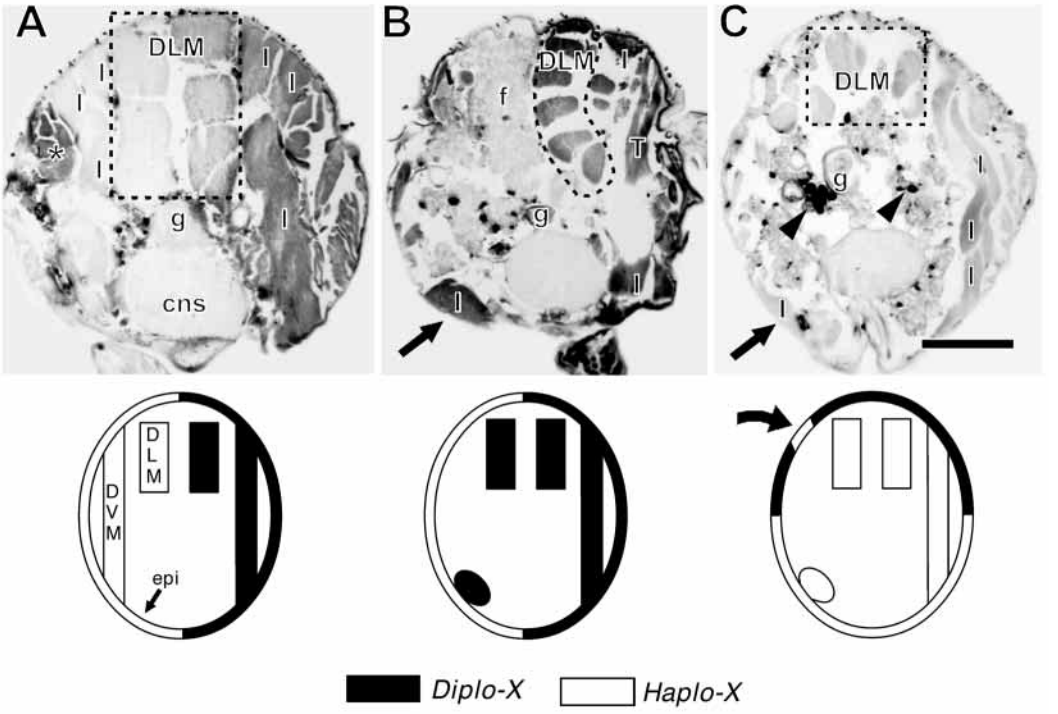

Fig. 3. βgal histochemistry of mosaic thoraces. Top row, frontal sections, dorsal is up. Bottom row, diagrams indicate the genotypes of the epidermis (epi), DLM and DVM (with diplo-*X* tissues in black), as well as the DVM phenotype (either attached or detached with a ventral remnant). The genotype assignments for the epidermis were based on direct observation of visible markers (*yellow*, *singed*) prior to tissue fixation, while muscle genotypes were based on the presence or absence of βgal enzymatic activity; see Materials and Methods for details. (A) Control mosaic (*y w sn*^{3}*/Mhc-lacZ; pal/+*). The epidermis of the left hemithorax is haplo-*X*, while the right is diplo-*X*. DVM I (I) and DLM (surrounded by dashed box) are βgal$^+$ (diplo-*X*) on the right, and βgal$^-$ (haplo-*X*) on the left. Note the βgal$^+$ direct flight muscles on the left (asterisk). (B) Experimental mosaic (*y rbp*^{5} *w*^{a} *sn*^{3}*/Mhc-lacZ; pal/+*). The epidermis of the left hemithorax is *rbp*^{5} (haplo-*X*) while that on the right is wild type (diplo-*X*). All muscles are βgal$^+$, and therefore genotypically wild type. The right DVM I, DLM and TTM (T) appear normal (most of DVM I is in another plane), whereas the left DVM I and DLM have detached, with DVM I leaving a βgal$^+$ remnant (arrow) in the ventral thorax. The left TTM has an abnormal dorsal attachment site in another plane of section. Note also that the space normally occupied by the IFM is filled by fat body (f). (C) Another experimental mosaic, in which all IFM are βgal$^-$ (and therefore *rbp*^{5}). Tissues expressing endogenous βgal stain strongly (arrowheads), indicating that histochemical staining was successful. On the right side, the dorsal epidermis is wild type, the ventral epidermis is mutant, and the DVM appear normal. On the left side, the ventral epidermis, and part of the dorsal EMA of DVM I (curved arrow in diagram) are mutant, and DVM I has detached and degenerated, leaving a small remnant in the ventral thorax (arrow). Because of fasciculation defects, the DLM have fewer fibers than normal, a common *rbp* phenotype, but those fibers occupy normal sites and overall DLM muscle bulk is comparable to that of wild type. Abbreviations: cns, central nervous system; g, gut. Bar, 100 μm.

muscle is dictated primarily by the genotypes of the muscles and/or EMAs, and not those of other tissues.

The most informative data came from the 45 muscle groups of experimental mosaics in which the DVM and their EMAs had different genotypes. The DVM showed a mutant phenotype in 90% of the cases in which the dorsal epidermis was mutant and the muscle and ventral EMA were wild type (n=10; Fig. 2A). This proportion does not differ from that in non-mosaic *rbp*^{5}*/Y* mutant DVM (P>0.5). The frequency of muscle defects was not increased (84%) when the ventral epidermis was also mutant (n=25; Figs 2A, 3B). Conversely, the majority of DVM were phenotypically normal when the dorsal and ventral epidermis were wild type and the muscle was mutant (n=5; Fig. 2A) or when the muscle and the ventral epidermis were mutant (n=5; Figs 2A, 3C). Both of these mosaic groups showed intermediate frequencies that were significantly different from both the wild type (P<0.02) and non-mosaic mutant (P<0.001). Thus, the data strongly suggest that the genotype of the dorsal EMA is critical for correct and stable DVM attachment, while those of the ventral EMA and the muscle itself have lesser importance.

The DVM of experimental mosaics in which clonal boundaries passed through or near the dorsal EMA (and were therefore not included in the quantitative analysis) provided additional support for this interpretation. Six of nine genotypically wild-type DVM failed to attach to partially mutant dorsal EMAs. For example, an *rbp*$^+$ DVM II fiber failed to attach to its correct EMA, which was about half wild type and half mutant. Instead, it made an ectopic contact with the posterior part of the adjacent wild-type EMA of the ipsilateral TTM. The TTM attachment was partially displaced, being crowded into the anterior portion of its own EMA (data not shown).

To determine the effects of (i) the epidermal markers *y* and *sn*^{3}, (ii) the *Mhc-lacZ* transgene, and (iii) *pal*-induced mosaicism, we examined 48 DVM from eight control (*y w sn*^{3}*/Mhc-lacZ*) mosaics. The great majority (46/48) of the DVM were phenotypically normal, regardless of the genotypes of the muscles or their EMAs (Figs 2A, 3A). Both abnormal DVMs were diplo-X. One, with diplo-X EMAs, had detached from the dorsal thorax. The other, with a haplo-X (*y*, *sn*^{3}) dorsal EMA and a diplo-X ventral EMA, was absent. Such defects were not observed in non-mosaic, wild-type controls, suggesting that *pal*-induced mosaicism may cause a low background level (<5%) of DVM defects. Consistent with these observations, Ewer et al. (1992) showed that some *pal* control mosaics inexplicably showed a mutant phenotype, perhaps because of heterozygosity for *pal* or hemizygosity for

the fourth chromosome. Nonetheless, in the present study, the effect of *rbp* mutant dorsal EMA on the DVM phenotype greatly exceeds the very low background frequency of abnormalities, supporting the hypothesis that the genotype of the dorsal epidermis is critical for the establishment and maintenance of normal DVM attachments.

DLM and TTM phenotypes in mosaics

DLM and TTM development are dependent on rbp^+ function, although to a lesser degree than for DVM (Restifo and White, 1992; Sandstrom et al., 1997). Therefore, analysis of the *pal*-induced mosaics was also used to identify the genetic focus of the DLM and TTM defects in *rbp* mutants. For DLM, the unit of analysis was the entire DLM on a given side, consisting of six fibers. Anterior and posterior DLM attachments are both located in the dorsal thorax. TTM were scored using the same criteria as for DVM. TTM and DLM defects were not observed in control mosaics, nor were they seen in non-mosaic controls (DLM: n=62 muscles, Fig. 2B; TTM: n=53 muscles, Fig. 2C).

In non-mosaic mutants (*y* rbp^5 w^a sn^3/Y; *pal*/+), 5 of 18 DLM had ectopically-attached fibers, consistent with previous observations (Sandstrom et al., 1997). In experimental mosaics, 3 of 10 wild-type DLM with mutant anterior and posterior EMAs showed ectopic attachments. None of the four mutant DLM with wild-type EMAs was defective. No wild-type DLM with wild-type EMAs contained ectopically attached fibers (n=14), and both mutant DLM with mutant EMAs were ectopically attached (Fig. 2B). In no case did anterior and posterior EMAs of a given DLM have different genotypes, so the relative contribution of anterior and posterior regions could not be assessed. These data indicate that correct attachment of the DLM requires rbp^+ function in the epidermis, although the requirement does not appear to be as stringent as it is for DVM.

Roughly half (5 of 9) of the TTM from non-mosaic rbp^5/Y; *pal*/+ mutant animals exhibited defects, including absent muscle, dorsal detachment, and ectopic dorsal attachment. However, among the 28 TTM that could be analyzed from mosaic thoraces, only two displayed defects, and both of these had mutant ventral EMAs (Fig. 2C). One of these was a mutant TTM that had detached dorsally from a wild-type EMA. The other was a wild-type TTM with an ectopic dorsal EMA; both of its EMAs were mutant. Ten of the 11 TTM with mutant dorsal EMAs were normal. Thus, while the small sample size precludes strong conclusions, the data suggest that rbp^+ function is not required in the dorsal epidermis for normal TTM attachment.

Ultrastructure of developing DVM and their attachments in wild type and *rbp* mutants

The analysis of mosaic thoraces described above showed that correct and stable DVM attachment requires rbp^+ function in the dorsal EMAs. To identify features of muscle attachment that are under rbp^+ control, we compared the ultrastructural morphology of the dorsal and ventral EMAs, the DVM, and the myotendinous junctions (MTJs) of wild-type and *rbp* mutant pupae. The goal was to identify defects in cellular differentiation that could explain the inability of *rbp* DVM to establish competent, stress-bearing attachments to the dorsal thorax, while they almost always make normal ventral attachments. We focused on DVM I because of the ease of generating longitudinal sections through it (Fig. 1) and because its development has been examined at the light microscopic level in wild type and in *rbp* mutants (Sandstrom et al., 1997). The strong hypomorphic lethal allele, rbp^1, was chosen for examination because it causes DVM defects in all animals, yet the great majority of mutants survive to the pharate adult stage (Restifo and White, 1992; Sandstrom et al., 1997).

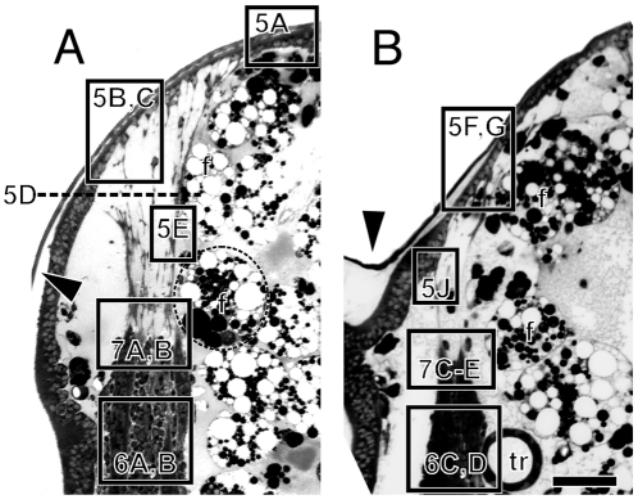

Fig. 4. Developing DVM and their dorsal EMAs in wild-type and mutant pupae, 14 hours after head eversion (HE + 14; ~26 hours APF). Frontal semi-thin plastic sections (approximately 1 μm), stained with toluidine blue, showing the dorsal end of DVM I, its dorsal EMA, and the epidermal tendon cell processes linking them. Dorsal is up, and regions corresponding to electron micrographs in Figs 5-7 are boxed. The horizontal plane of the section shown in Fig. 5D is indicated by a dashed line. In both genotypes, apolysis has occurred and the pupal cuticle (arrowheads) has largely separated from the apical membrane of the epidermal cells that secreted it; the adult cuticle has not yet been secreted. (A) Canton-S. The muscle (box 6A,B) is linked to the EMA (box 5B,C) via a dense array of tendon cell processes (box 7A,B). Dashed circle demarcates the extent of a single fat body cell (f), many of which are visible. (B) rbp^1/Y. Although DVM I (box 6C,D) appears grossly normal, its dorsal end is extremely narrow and is linked to the EMA (box 5F,G,I) by an abnormally small number of processes (box 7C-E). tr, trachea. Bar, 10 μm.

In the wild-type pupa 14 hours after head eversion (HE+14, approximately 26 hours after puparium formation), fusion of adepithelial cells is well underway, giving rise to three distinct DVM fibers. The fibers have shortened and are suspended by an array of long processes, each extending from a tendon cell in the dorsal or ventral attachment sites (Fig. 4A; Shatoury, 1956; Fernandes et al., 1991; Sandstrom et al., 1997). At the same stage in *rbp* mutants, DVM are still attached to the dorsal epidermis, although the connecting material is sparse (Fig. 4B). In general, medial connections are disrupted first, leaving the mutant muscles leaning against the lateral thoracic wall. The dorsal ends of the muscles are narrower than in the wild type (Fig. 4B), while the ventral ends appear normal (data not shown). By six hours later (HE+20), most of the mutant DVM fibers have detached from the dorsal thorax (Sandstrom et al., 1997). Therefore, the transmission electron microscopy study was performed at HE+14, when the mutant muscles, tendon

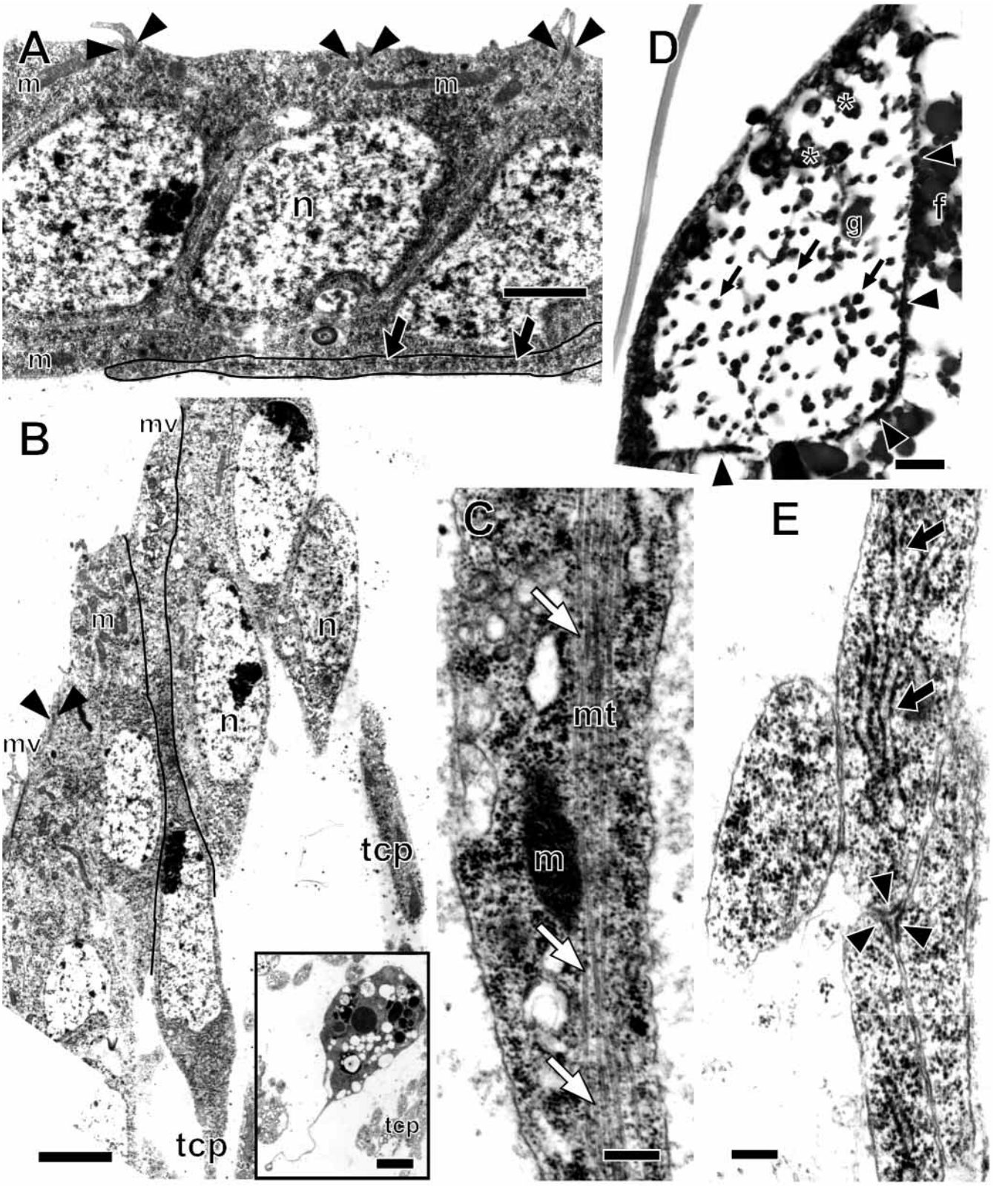

Fig. 5

cells and their connections are at maximum maturity without obvious evidence of degeneration. The light micrographs in Fig. 4 are labeled as a guide to the electron micrographs presented below.

The EMA and surrounding epidermis

Three cell types are readily distinguished in electron micrographs of the pupal thoracic body wall: patches of EMA cells in characteristic locations, non-EMA epidermis, and

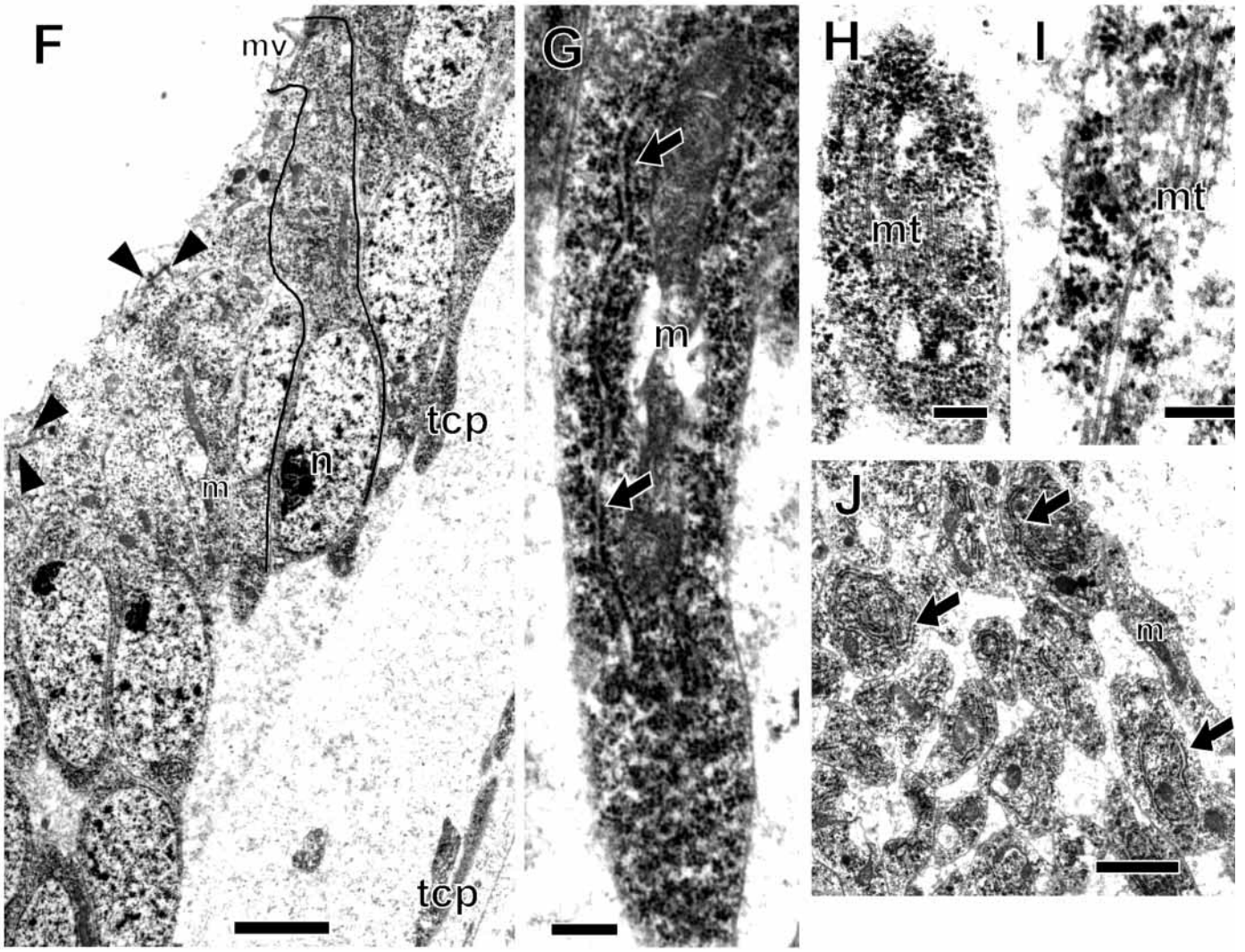

Fig. 5. Structure of the thoracic epidermis, including tendon cell processes and sheath, in wild-type and mutant pupae. Electron micrographs unless otherwise indicated. (A) Canton-S non-EMA epidermis, HE+14, dorsomedial to the DVM I EMA (15,000×). Epidermal cells contain extensive rough ER (large arrows), and are connected by zonulae adherens (arrowheads) at their apical ends. At their basal surfaces, the cells produce broad cytoplasmic extensions, directed toward the EMA. One such extension, originating from a cell outside the field of view, is outlined. (B) Canton-S DVM I EMA cells HE+14 (5,000×). Like the non-EMA epidermis, the apical ends of these long, fusiform cells have microvilli (mv), zonulae adherens, and extensive rough ER. Along their basolateral margins the EMA cells separate from their neighbors and extend slender tendon cell processes (tcp) toward the muscle. The lateral contacts between one EMA cell and its neighbors are outlined. Inset: phagocytic hemocyte within the region bounded by sheath (5,000×). Note its diverse inclusions and long, narrow process. (C) Canton-S dorsal EMA, HE + 14 (15,000×). This process has been sectioned longitudinally, revealing a large bundle of microtubules (mt; white arrows) extending toward the developing MTJ. (D) Canton-S, HE+14, light micrograph of horizontal paraffin section. Lateral is to the left; anterior is up. The sheath (arrowheads) completely encircles the tendon cell processes (some indicated by small arrows). Clusters of tendon cell nuclei are indicated by asterisks. Although a fat globule (g) moved into the region during staining or sectioning, intact fat body cells (f) are never observed within the region, despite being common just outside (e.g. Fig. 4). (E) Canton-S, HE+14, a small region of the sheath, longitudinal section (40,000×). Overlapping cytoplasmic extensions, originating from an unknown cell type, are joined by spot adherens junctions (arrowheads) and contain extensive rough ER (large arrows). (F) *rbp*^{1}, HE+14, DVM I EMA (5,000×). As in the wild type, mutant EMA cells are linked by apical zonulae adherens and contain extensive rough ER. They are also elongated, shown by the outline of one cell, and extend processes, although these are less common than in the wild type. (G) *rbp*^{1}, dorsal EMA, HE + 14 (15,000×). Although rough ER (large arrows) and mitochrondria (m) are evident, microtubule bundles are not present. (H) *rbp*^{1} mutant, ventral EMA, HE + 14 (15,000×). Unlike in the dorsal EMA of comparable animals, prominent bundles of microtubules (mt) are present. (I) *rbp*^{1}, dorsal EMA, at a later stage of development, HE + 20 (40,000×). Microtubules are readily discerned. (J) *rbp*^{1}, HE+14, electron micrograph of cellular material ventrolateral to the dorsal DVM I EMA (15,000×). The membrane-bound profiles, originating from an unknown cell type, contain extensive rough ER (large arrows) and mitochondria (m), but no microtubules. n, nucleus. Bars: (A,J) 1 μm; (B,F) 2 μm; (C,G) 500 nm; (E,H,I) 200 nm; (D) 5 μm.

scattered clusters of developing trichoid sensillae (Hartenstein and Posakony, 1989; Reedy and Beall, 1993b). We focused on the first two, which share characteristic features of insect epidermis (Poodry, 1980; Tepass and Hartenstein, 1994), including extensive rough endoplasmic reticulum (RER), apical microvilli, and zonulae adherens (ZA) linking

neighboring cells just below their apical surfaces (Fig. 5A,B). ZA are visible as short stretches of electron-dense material in adjacent cell membranes and lighter material in the intervening extracellular space (Tepass and Hartenstein, 1994).

Cells of non-EMA epidermis are uniform in size and shape and make full side-to-side contact

with their neighbors, forming a simple columnar epithelium whose nuclei all lie at approximately the same level (Fig. 5A). The basal membrane of each non-EMA epidermal cell is drawn out into a sheetlike protrusion containing much RER and directed toward the EMA (Fig. 5A). Each protrusion extends along and partially overlaps those of several neighboring cells. Because non-EMA epidermis was not exhaustively sampled, we do not know whether all the cells have such basal extensions at this stage of development.

In contrast, EMA cells, all of which are likely to be epidermal tendon cells, show marked variation in size and shape, forming a pseudostratified columnar epithelium (Fig. 5B). The cells are generally fusiform, contacting their neighbors primarily along their apical margins, where they are secured by ZA, and then separating at more basal locations. These features, in combination with nuclei lying at many different levels, result in an overall disorderly appearance. In extreme cases, the cells appear stretched, with a stalk-like apical portion, and the nucleus residing tens of microns away from the apical surface (Fig. 5B). The basal end of each EMA cell tapers into a slender process (Fig. 5B) that extends over 100 μm to contact the shortened DVM (Fig. 4A). Microtubule bundles are a prominent feature of tendon cell processes along their entire length (Fig. 5C), and can also be seen throughout the EMA cell body, parallel to its long axis. With the exception of cells presumed to be developing sensillae (data not shown), all cells in a given thin section of the EMA had one or more tendon cell characteristics. Hence, we believe they were all tendon cells, although serial section reconstruction would be required to determine if all of them possess all features.

The array of tendon cell processes from each EMA site is surrounded by a cylindrical sheath composed of an unknown cell type (Fig. 5D,E). This structure, which has not been described previously, appears to form a selective exclusion barrier around the bundle of tendon cell processes. For example, fat body cells, which are numerous throughout the pupal thorax, are not present among the processes (Fig. 4A). In contrast, this zone frequently contains phagocytic hemocytes (Fig. 5B, inset), important mediators of tissue reconstruction during metamorphosis (Kurata et al., 1992; Rheuben, 1992; Cantera and Technau, 1996). Ultrastructurally, the sheath is composed of several flattened, overlapping, membranous extensions joined by spot adherens junctions, occassionally with a triad organization (Fig. 5E). RER is abundant within the cytoplasm, but no microtubules or other cytoskeletal elements were observed (Fig. 5E). While we could not identify the cell bodies whose extensions comprise the sheath, the qualitative similarities to the extensions of non-EMA epidermis suggest that a ring of these cells, surrounding the EMA, may be the source.

In *rbp*^{1} pupae at HE+14, the DVM I EMA can be recognized in appropriate locations of the dorsal thoracic epidermis, but their cells lack critical hallmarks of differentiation (Fig. 5F). Like those of wild type, mutant dorsal EMAs contain fusiform

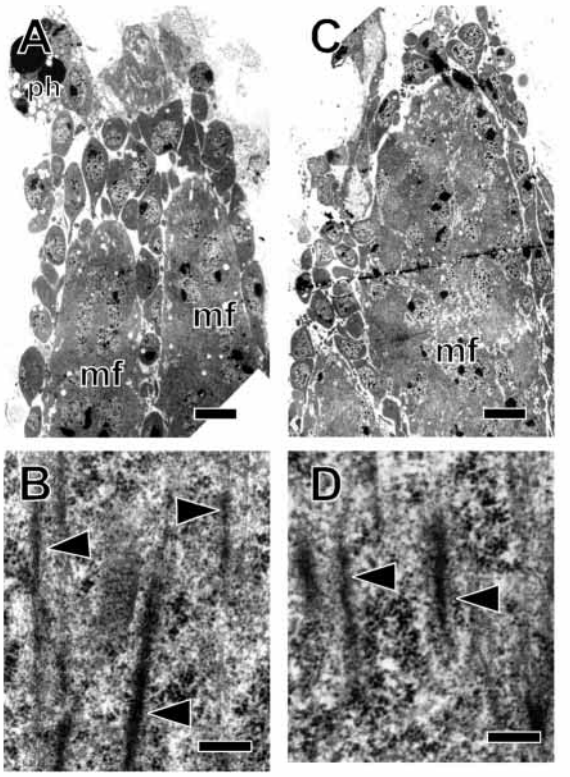

Fig. 6. Electron micrographs of DVM I in wild-type and mutant pupae, HE + 14. (A) Canton-S, oblique section through the muscle, showing two of the three developing multinucleate muscle fibers (mf) surrounded by numerous myoblasts (2,500×). A phagocytic hemocyte (ph) appears to be engulfing an unfused myoblast. (B) Canton-S, higher magnification view of muscle fiber cytoplasm (45,000×). Fibrous elements (arrowheads), believed to be incipient myofibrils, are common. (C) *rbp*^{1}, oblique section through developing multinucleate muscle fibers, surrounded by myoblasts, similar to the wild type (2,500×). The straight dark line crossing the image is a sectioning artifact. (D) Higher magnification view of *rbp*^{1} muscle fiber cytoplasm (40,000×). Longitudinally-oriented fibrous material (arrowheads) is apparent, as in the wild type. Bars: (A,C) 5 μm; (B,D) 500 nm.

cells that are connected apically by ZA and are separated from their neighbors along much of their lengths. However, few processes extend from these tendon cells toward the muscle, and the processes that are seen lack microtubule bundles (Fig. 5G). In contrast, at the same developmental stage, the ventral EMA of *rbp*^{1} shows numerous tendon cell processes filled with microtubules (Fig. 5H). Therefore, *rbp*^{1} pupae are not simply globally delayed in their development.

Six hours later (HE+20, approximately 32 hours after puparium formation), the few mutant tendon cell processes extending from the dorsal EMA do contain microtubule bundles (Fig. 5I). By this time, however, most of the DVM muscle fibers have already detached from the dorsal thorax. Thus, the *rbp*^{1} dorsal EMA manifests delayed or incomplete tendon cell differentiation, specifically of the tendon cell processes, the very components responsible for securing the ends of DVM fibers.

Adjacent to the *rbp*^{1} dorsal EMA are large, jumbled collections of RER-filled, membrane-bound material connected

by spot adherens junctions (Fig. 5J). This material appears to represent remnants of the cylindrical sheath that normally surrounds the tendon cell processes. Lower magnification views reveal that the sheath of *rbp[1]* mutants, surrounding the sparse and defective tendon cell processes, is aberrant, with numerous gaps especially along the medial side (see Fig. 7C).

Muscle fibers

In the wild-type pupa at HE+14, the three multinucleate DVM I fibers are each surrounded by imaginal myoblasts, presumably in the process of fusing with the developing muscle (Fig. 6A). The cytoplasm of myoblasts and muscle fibers share ultrastructural characteristics, including numerous ribosomes and small mitochondria. Unique to the muscles, however, are arrays of fibrous elements running parallel to the long axis of the muscle (Fig. 6B). In some sections, these fibrous elements are flanked by microtubules. Based on ultrastructural analysis of DLM development (Reedy and Beall, 1993a) and the expression of MHC in the IFM at this stage (Fernandes et al., 1991), the fibrous elements are likely to represent the earliest stage of DVM myofibril assembly.

In *rbp[1]* pupae, the three DVM I fibers appear to be normal in length and bulk and are surrounded by a normal-appearing population of myoblasts (Fig. 6C). Nuclear and cytoplasmic features of the muscle fibers, including the parallel arrays of fibrous elements, are similar to those in wild type (Fig. 6D). Thus, the only detectable abnormality of the mutant muscle fibers is that seen at the light microscopic level, namely the marked tapering at their dorsal ends (Figs 4B, 7E). In contrast, the ventral ends of *rbp[1]* muscle fibers have a normal contour, slightly convex with no significant tapering (data not shown). Because the mutant muscle lacks ultrastructural defects, the gross morphological defect at the dorsal end is most likely a secondary consequence of the dramatic reduction in the area of contact between muscle fibers and the tendon cells forming the dorsal MTJ.

Myotendinous junctions

The wild-type contact zone between DVM I and epidermal tendon cells (Fig. 7A) is notable for an intimate association between the basal ends of numerous, densely packed tendon cell processes and the muscle fiber membrane. In most regions of contact, the muscle membrane is deeply convoluted and the tendon cell processes interdigitate with finger-like extensions of the muscle. There is variation in the degree of membranous convolutions, with some tendon cell processes contacting

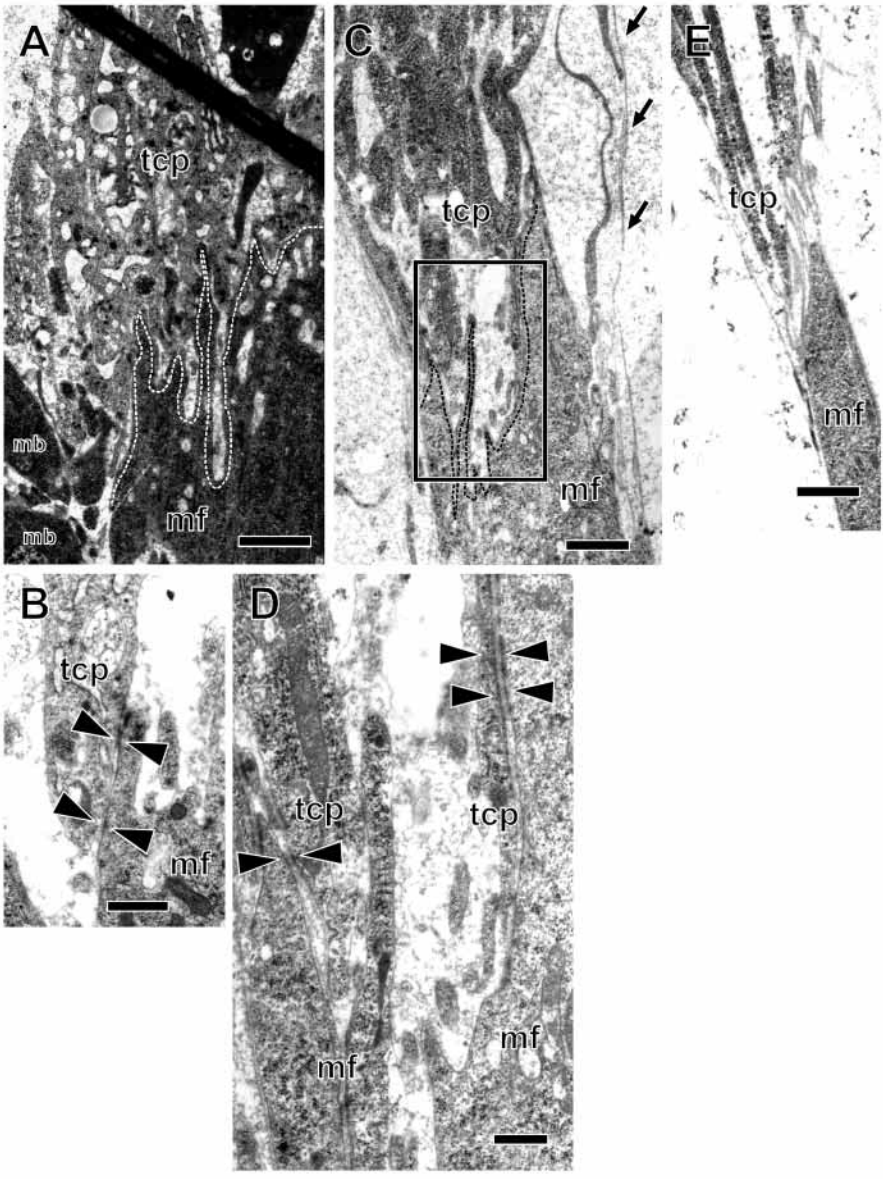

Fig. 7. Electron micrographs of DVM I dorsal myotendinous junctions (MTJs) in wild-type and mutant pupae, HE + 14. (A) Canton-S. Approximately half of the MTJ of this fiber is shown (5,000×). The basal ends of tendon cell processes (tcp) coalesce at the MTJ, appearing as a mass covering the ends of the muscle fiber (mf). The convoluted interface between the tcp and muscle is highlighted by the dashed line parallel to the muscle fiber membrane. The straight diagonal line in the upper right is a histological artifact. (B) Canton-S, higher magnification view of a contact between tendon cell process and muscle (13,000×). Spot adherens junctions (arrowheads) have formed, but are not associated with cytoskeletal specializations in either the muscle or tcp. (C) Moderately affected *rbp[1]* (5,000×), showing the full extent of the MTJ of this fiber. The muscle (mf) and tendon cell process (tcp) membranes interdigitate, but the junction is less complex than are wild-type junctions. Shreds of material, possibly remnants of the sheath, are indicated by arrows. (D) Higher magnification view of the boxed region in (C) (15,000×). Spot adherens junctions (arrowheads) are seen between the muscle fiber and tendon cell processes. (E) A more severely affected *rbp[1]* MTJ (5,000×). The muscle comes to a very narrow, smooth point, rather than being broad and convoluted at its dorsal end, and is linked to tendon cell processes via strands of unidentifiable material. mb, myoblast. Bars: (A,C,E) 2 μm; (B,D) 500 nm.

smooth segments of muscle membrane. The apposition of muscle and tendon cell membranes is reinforced by many spot adherens junctions (Fig. 7B), but we observed no cytoskeletal specializations associated with the muscle-epidermal contacts. The ventral MTJ has a similar appearance (data not shown). The spot adherens junctions visible at this stage may represent the initial step in the differentiation of the mature MTJ, a massive structure containing specializations of cytoskeleton, membrane and extracellular matrix (Auber, 1963; Ready and Beall, 1993b).

The dorsal MTJs of *rbp*^{1} mutants are clearly defective, with variable severity among the individuals sampled (Fig. 7C-E). At the mild end of the spectrum, the area of muscle-tendon contact is greatly reduced, although the muscle and tendon cell membranes do interdigitate and form spot adherens junctions (Fig. 7C,D). The diminished contact between muscle and tendon cells is consistent with the markedly reduced numbers of tendon cell processes extending from the dorsal EMA some distance away. Mutant MTJs never show the extensive interdigitations commonly seen at wild-type MTJs. At the most aberrant MTJs, small numbers of tendon cell processes are tenuously linked to the muscle by strands of material that could be extracellular matrix or cellular debris (Fig. 7E). This extreme phenotype reflects either minimal differentiation of the dorsal EMA or early stages of muscle detachment. None of the *rbp*^{1} dorsal MTJs examined in this study appeared capable of maintaining muscle attachment, consistent with the low frequency of DVM survival in these mutants (Restifo and White, 1992; Sandstrom et al., 1997). In striking contrast, however, all ventral MTJs of *rbp*^{1} at this stage appear normal (data not shown).

DISCUSSION

The goals of this study were to determine where *rbp*$^{+}$ function is required for IFM attachment and to identify cellular mechanisms of the *rbp* IFM phenotypes. *rbp*$^{+}$ represents one of three distinctive functions encoded by *BRC*, an essential transducer of 20E action during metamorphosis (Bayer et al., 1996b). Our findings, based on analysis of genetic mosaics and ultrastructural examination, allow us to propose molecular links between the ecdysone cascade regulating adult morphogenesis and the cell-cell interactions previously shown to underlie embryonic muscle attachment in *Drosophila*.

Site of action of *rbp*$^{+}$

The mosaic analysis revealed that *rbp*$^{+}$ function is required in the dorsal EMA for normal DVM attachment. In *rbp* mosaics, when the dorsal EMA was mutant, the frequency of DVM attachment defects was very high, and not different from that seen in completely mutant animals. Conversely, mutant DVM muscle fibers with wild-type dorsal EMAs had infrequent aberrant dorsal attachments. Furthermore, in both types of mosaics, the presence of mutant ventral EMA tissue did not enhance the DVM attachment phenotypes. In other words, the genotype of the dorsal EMA was the strongest predictor of DVM phenotype. If the muscle fibers themselves make a contribution to the DVM phenotype, it is a modest one. This result adds to findings from surgical, biochemical and genetic manipulations demonstrating the importance of the epidermis in development and survival of the associated musculature (Poulson, 1945; Williams and Caveney, 1980; Volk and VijayRaghavan, 1994; Baker and Schubiger, 1995; VijayRaghavan et al., 1996; Halfon and Keshishian, 1998).

The data further indicate that DVM degeneration in *rbp* mutants is a secondary result of detachment, and that *rbp*$^{+}$ function is not required for muscle maintenance. We previously showed that *rbp* mutant DVM that remain attached at both ends develop to apparent maturity, while almost all detached DVM undergo degeneration (Sandstrom et al., 1997). In the *rbp* mosaics, both mutant and wild-type detached muscles underwent degeneration, and many of each genotype disappeared altogether, while mutant DVM that maintained attachments appeared completely normal. Hence, *rbp*$^{+}$ function could not rescue detached muscles, nor was it required for survival of attached muscles. The detachment-induced degeneration observed in *rbp* mutants is reminiscent of a phenomenon long studied in vertebrates, in which tendon transection causes muscle atrophy and degeneration (Eccles, 1944; Karpati et al., 1972; Margolis and Baker, 1983).

Our mosaic analysis also rules out significant involvement of the central nervous system (CNS) in *rbp* muscle phenotypes, in spite of CNS defects in *rbp* mutants (Restifo and White, 1991) and evidence that innervation plays a critical role in DVM development (Fernandes and Keshishian, 1998). While we did not have CNS genotype markers, the question can be addressed by considering the blastoderm fate map and the *pal* mechanism. The thoracic ganglia innervate the IFM (Coggshall, 1978; Ikeda and Koenig, 1988; Fernandes and VijayRaghavan, 1993) and arise from embryonic cells very close to precursors of the adult ventral thoracic epidermis (Hartenstein et al., 1985; Lawrence and Johnston, 1986). Because *pal* induces chromosome loss very early (Baker, 1975), the ventral epidermis and thoracic ganglia of mosaics are highly likely to share the same genotype. Thus, if *rbp*$^{+}$ function were required in the CNS for DVM attachment, DVM defects would be strongly associated with ventral epidermis genotype, but this was not the case.

Selective vulnerability of DVM dorsal EMAs

The dorsal EMAs of the DVM are preferentially sensitive to *rbp* mutations, even though (i) dorsal MTJs develop with the same time course as their ventral counterparts, and (ii) BRC-Z1, the primary mediator of *rbp*$^{+}$ function (Crossgrove et al., 1996; Bayer et al., 1997; Sandstrom et al., 1997), is distributed uniformly throughout the thoracic epidermis at the stage when it rescues *rbp* muscle phenotypes (Sandstrom et al., 1997). *BRC* mutations affect other structures with dorsal selectivity as well. In the oocyte, the dorsal phenotype can be explained by localized *BRC* expression (Huang and Orr, 1992; Deng and Bownes, 1997). In the optic lobe, *BRC* expression appears equal in affected and unaffected cells (Liu and Restifo, 1998), so other features must distinguish dorsal and ventral counterparts of similar regions. In the developing DVM, distinguishing factors may include the geometry of the EMAs or signaling between EMA and muscle at dorsal and ventral attachment sites (see below).

EMAs of *rbp* mutant DLM are much less affected than those of DVM. Previously we suggested (Restifo and White, 1992) that the DVM predominance of the *rbp* phenotype relates to the distinct developmental strategies of two types of IFM, with DLM using a larval muscle template and DVM constructed de novo

(Shatoury, 1956; Costello and Wyman, 1986; Fernandes et al., 1991). However, our current findings reveal that the differential genetic susceptibility resides in their dorsal EMAs, rather than in the muscles per se.

Structural correlates of *rbp* attachment defects

Electron microscopic examination corroborates the results of the mosaic analysis, showing specific defects of *rbp* mutant dorsal EMA cells at DVM attachment sites, while the muscle fibers appear normal. All epidermal cells in the mutant EMA have ultrastructural features of tendon cells, e.g. fusiform shape. Similarly, ubiquitous expression of BRC-Z1 completely rescues the *rbp* muscle attachment phenotypes without inducing ectopic EMAs (Sandstrom et al., 1997). These data demonstrate that specification of tendon cell fate is not under rbp^+ control.

Subsequent events in tendon cell and MTJ differentiation, however, are disrupted in *rbp* mutants. Very few tendon cell processes connect the dorsal EMA to the DVM fibers, and the MTJ has reduced surface area and complexity. The few tendon cell-muscle contacts can form normal-appearing adherens junctions, but the microtubule bundles that are characteristic of tendon cells appear late. The sheath around the sparsely populated tendon cell process region is incomplete, either due to retarded development or mechanical damage from the abnormal position of the muscle as the fibers start to detach. Detachment occurs during the period of muscle shortening, concurrent with the first appearance of immature myofibrils. The mechanism and function of muscle shortening are unknown, but it does not require Myosin heavy chain (Sandstrom et al., 1997). In the wild type, the tendon cell processes elongate and maintain connection with the shortened muscle fibers. In *rbp* mutants, the small number of incompletely differentiated tendon cell processes can not withstand the mechanical stress of muscle shortening, and/or can not elongate, and the processes break. Thus, muscle shortening provides the proximate trigger for DVM detachment and subsequent degeneration, but the primary defect is the developmental failure of the dorsal EMA cells.

The rbp^+ dorsal EMA also guides muscle fibers to correct attachment sites. A particularly striking feature of the *rbp* phenotype is the invasion by DLM of DVM EMAs while they are still occupied by DVM (Sandstrom et al., 1997), a clear indication that DVM EMAs are overly 'attractive' even though they are defective. Because there are no ultrastructural differences between wild-type EMAs of DVM and DLM (this study; Reedy and Beall, 1993b), we suggest that they express different molecular labels. An imbalance in the blend of attractive and repulsive cues that normally guide migrating muscles could then explain the ectopic attachments seen in *rbp* mutants.

This study revealed a previously undescribed sheath of overlapping flattened cytoplasmic extensions surrounding the tendon cell processes. The sheath defines a distinct compartment, and may function to exclude cells and other material that could interfere with subsequent re-extension of the muscle. Muscle shortening, tendon cell processes, and the sheath represent special features of IFM and TTM development that are not seen during embryonic muscle attachment (Tepass and Hartenstein, 1994; Bate et al., 1999). They may have parallels with wing morphogenesis, during which two cell layers undergo separation and subsequent apposition (Fristrom et al., 1993).

The ecdysone cascade and the molecular basis of muscle attachment

We propose that transcription factor BRC-Z1, induced by 20E in the thoracic body wall, regulates a number of target genes whose products control specific features of tendon cell maturation. It is likely that intercellular signaling mechanisms are shared during embryonic and adult muscle attachment, just as neural cell fate determination is controlled similarly at both stages (Goriely et al., 1991; Modolell, 1997). In the embryo, muscle-independent expression of the transcription factor Stripe induces EMA specification and initital differentiation (Volk and VijayRaghavan, 1994; Lee et al., 1995; Frommer et al., 1996; Becker et al., 1997; Vorbrüggen and Jäckle, 1997). During metamorphosis, Stripe is expressed in the EMAs of the IFM and TTM, initially in a muscle-independent manner (Fernandes et al., 1996; Sandstrom et al., 1997). Viable *stripe* mutations disrupt IFM development (Costello and Wyman, 1986; de la Pompa, 1989). PS integrins, which play an essential role in muscle attachment by linking the extracellular matrix to the cytoskeleton (Longhurst and Jennings, 1998), are expressed at developing EMAs in both embryos and pupae (Newman and Wright, 1981; Bogaert et al., 1987; de la Pompa et al., 1989; Drysdale et al., 1993; Fernandes et al., 1996; Prokop et al., 1998). Thus, studies of embryonic muscle attachment provide a useful framework for understanding mechanisms of BRC-Z1 action in the dorsal thoracic EMAs.

The muscle-independent phase of *stripe* expression, which in the embryo induces *short stop* (previously known as *groovin* or *kakapo*; Volk and VijayRaghavan, 1994; Prout et al., 1997; Strumpf and Volk, 1998) and *alien* (Becker et al., 1997; Vorbrüggen and Jäckle, 1997; Yarnitzky et al., 1997), is also *rbp*-independent in the pupal thorax. *stripe* expression in imaginal discs precedes the rise of BRC-Z1 (Emery et al., 1994; Bayer et al., 1996a) and expression in early pupal EMAs is normal in *rbp* mutants (DJS, unpublished), consistent with normal tendon cell specification.

It is therefore more likely that rbp^+ function promotes a muscle-dependent phase of tendon cell differentiation. Embryonic muscle secretes the neuregulin-like molecule Vein, a signal received by the EGF receptor (Egfr/DER; Shilo and Raz, 1991) in the epidermis, resulting in expression of EMA-specific markers β1 tubulin and the bHLH protein Delilah and further up-regulation of Stripe, Short stop and Alien (Armand et al., 1994; Buttgereit, 1996; Yarnitzky et al., 1997). Hence, candidate target genes for BRC-Z1 in the pupal EMA include *Egfr*, *delilah*, *β1 tubulin*, *short stop*, *alien* and *stripe*. The recent finding that Alien may be a co-repressor for the ecdysone receptor (Dressel et al., 1999) suggests the additional possibility that BRC-Z1 overcomes Alien-mediated transcriptional repression, thereby unleashing the ecdysone cascade in pupal thoracic epidermis.

We thank Patty Jansma for generous assistance with sample preparation, Gina Zhang for cutting the plastic sections, C. Hedgcock, R.B.P., for printing the electron micrographs, Dave Bentley for advice on electron microscopy, Nirav Merchant and Terrill Yuhas for help with computer graphics, Mary Reedy (Duke U.) for helpful suggestions, Sandy Bernstein and Jeff Hall for stocks, John Ewer (Cornell U.) for advice on use of *pal*, Dianne Fristrom and Sharon Hesterlee for thoughtful comments on the manuscript, Nick Strausfeld for use of the digital camera, and members of the Restifo lab for helpful discussions. This work was funded by grants to D.J.S. from the Small Grant Program (sponsored by the U. of Arizona Foundation and the Office of the Vice

President for Research) and to L.L.R. from NIH (NS28495). D.J.S. was supported in part by NIH Research Training Grant AI07475. This work and the interpretations in this article are those of the authors alone.

REFERENCES

Anand, A., Fernandes, J., Arunan, M. C., Bhosekar, S., Chopra, A., Dedhia, N., Sequiera, K., Hasan, G., Palazzolo, M. J., VijayRaghavan, K. and Rodrigues, V. (1990). *Drosophila* 'enhancer trap' transposants: gene expression in chemosensory and motor pathways and identification of mutants affected in smell and taste ability. *J. Genet.* **69**, 151-168.

Armand, P., Knapp, A. C., Hirsch, A. J., Wieschaus, E. F. and Cole, M. D. (1994). A novel basic helix-loop-helix protein is expressed in muscle attachment sites of the *Drosophila* epidermis. *Mol. Cell. Biol.* **14**, 4145-4154.

Ashburner, M. (1989). Drosophila: *A Laboratory Handbook.* Cold Spring Harbor, NY: Cold Spring Harbor Laboratory Press.

Auber, J. (1963). Ultrastructure de la jonction myo-épidermique chez les diptères. *J. Microscopie* **2**, 325-336.

Bainbridge, S. P. and Bownes, M. (1981). Staging of the metamorphosis of *Drosophila melanogaster*. *J. Embryol. Exp. Morphol.* **66**, 57-80.

Baker, B. S. (1975). *paternal loss* (*pal*): a meiotic mutant in *Drosophila melanogaster* causing loss of paternal chromosomes. *Genetics* **80**, 267-296.

Baker, R. and Schubiger, G. (1995). Ectoderm induces muscle-specific gene expression in *Drosophila* embryos. *Development* **121**, 1387-1398.

Bate, M. (1993). The mesoderm and its derivatives. In *The Development of* Drosophila melanogaster (ed. M. Bate and A. Martinez-Arias), pp. 1013-1090. Cold Spring Harbor, NY: Cold Spring Harbor Laboratory Press.

Bate, M., Landgraf, M. and Gomez-Bate, M. R. (1999). Development of larval body wall muscles. In *Neuromuscular Junctions in* Drosophila (ed. V. Budnik and L. S. Gramates), pp. 25-44. San Diego, CA: Academic Press. [alt: Int. Rev. Neurobiol.] **43**, 25-44.

Bayer, C. A., Holley, B. and Fristrom, J. W. (1996a). A switch in *Broad-Complex* zinc-finger isoform expression is regulated post-transcriptionally during the metamorphosis of *Drosophila* imaginal discs. *Dev. Biol.* **176**, 166-184.

Bayer, C. A., von Kalm, L. and Fristrom, J. W. (1996b). Gene regulation in imaginal disc and salivary gland development during *Drosophila* metamorphosis. In *Metamorphosis: Postembryonic Reprogramming of Gene Expression in Amphibian and Insect Cells* (ed. L. I. Gilbert, J. R. Tata and B. G. Atkinson), pp. 322-361. Academic Press, San Diego.

Bayer, C. A., von Kalm, L. and Fristrom, J. W. (1997). Relationships between protein isoforms and genetic functions demonstrate functional redundancy at the *Broad-Complex* during *Drosophila* metamorphosis. *Dev. Biol.* **187**, 267-282.

Becker, S., Pasca, G., Strumpf, D., Min, L. and Volk, T. (1997). Reciprocal signaling between *Drosophila* epidermal muscle attachment cells and their corresponding muscles. *Development* **124**, 2615-2622.

Bernstein, S. I., O'Donnell, P. T. and Cripps, R. M. (1993). Molecular genetic analysis of muscle development, structure, and function in *Drosophila*. *Int. Rev. Cytol.* **143**, 63-152.

Bogaert, T., Brown, N. and Wilcox, M. (1987). The Drosophila PS2 antigen is an invertebrate integrin that, like the fibronectin receptor, becomes localized to muscle attachments. *Cell* **51**, 929-940.

Buttgereit, D., Leiss, D., Michiels, F. and Renkawitz-Pohl, R. (1991). During *Drosophila* embryogenesis the *beta 1 tubulin* gene is specifically expressed in the nervous system and the apodemes. *Mech. Dev.* **33**, 107-118

Buttgereit, D. (1996). Transcription of the β1 tubulin (βTub56D) gene in apodemes is strictly dependent on muscle insertion during embryogenesis in Drosophila melanogaster. *Eur. J. Cell Biol.* **71**, 183-191.

Callahan, C. A., Bonkovsky, J. L., Scully, A. L. and Thomas, J. B. (1996). *derailed* is required for muscle attachment site selection in *Drosophila*. *Development* **122**, 2761-2767.

Campos, A. R., Grossman, D. and White, K. (1985). Mutant alleles at the locus *elav* in *Drosophila melanogaster* lead to nervous system defects. A developmental-genetic analysis. *J. Neurogenet.* **2**, 197-218.

Cantera, R. and Technau, G. M. (1996). Glial cells phagocytose neuronal debris during the metamorphosis of the central nervous system in *Drosophila melanogaster*. *Dev. Genes Evol.* **206**, 277-280.

Caveney, S. (1969). Muscle attachment related to cuticle architecture in Apterygota. *J. Cell Sci.* **4**, 541-559.

Chao, A. T. and Guild, G. M. (1986). Molecular analysis of the ecdysterone-inducible 2B5 'early' puff in *Drosophila melanogaster*. *EMBO J.* **5**, 143-150.

Coggshall, J. C. (1978). Neurons associated with the dorsal longitudinal flight muscles of *Drosophila melanogaster*. *J. Comp. Neurol.* **177**, 707-720.

Costello, W. J. and Wyman, R. J. (1986). Development of an indirect flight muscle in a muscle-specific mutant of *Drosophila melanogaster*. *Dev. Biol.* **118**, 247-258.

Crossgrove, K., Bayer, C. A., Fristrom, J. W. and Guild, G. M. (1996). The *Drosophila Broad-Complex* early gene directly regulates late gene transcription during the ecdysone-induced puffing cascade. *Dev. Biol.* **180**, 745-758.

de la Pompa, J. L., Garcia, J. R. and Ferrus, A. (1989). Genetic analysis of muscle development in *Drosophila melanogaster*. *Dev. Biol.* **131**, 439-454.

Deng, W.-M. and Bownes, M. (1997). Two signaling pathways specify localised expression of the *Broad-Complex* in *Drosophila* eggshell. *Development* **124**, 4639-4647.

DiBello, P. R., Withers, D. A., Bayer, C. A., Fristrom, J. W. and Guild, G. M. (1991). The *Drosophila Broad-Complex* encodes a family of related proteins containing zinc-fingers. *Genetics* **129**, 385-397.

Dickinson, M. H. and Tu, M. S. (1997). The function of dipteran flight muscle. *Comp. Biochem. Physiol.* **116A**, 223-238.

Dressel, U., Thormeyer, D., Altincicek, B., Paululat, A., Eggert, M., Schneider, S., Tenbaum, S. P., Renkawitz, R. and Baniahmad, A. (1999). Alien, a highly conserved protein with characteristics of a corepressor for members of the nuclear hormone receptor superfamily. *Mol. Cell. Biol.* **19**, 3383-3394.

Drysdale, R., Rushton, E. and Bate, M. (1993). Genes required for embryonic muscle development in *Drosophila melanogaster*. *Roux's Arch. Dev. Biol.* **202**, 276-295.

Eccles, J. C. (1944). Investigations on muscle atrophies arising from disuse and tenotomy. *J. Physiol.* **103**, 253-266.

Elgin, S. R. and Miller, D. W. (1978). Mass rearing of flies and mass production and harvesting of eggs. In *The Genetics and Biology of* Drosophila (ed. M. Ashburner and T. R. F. Wright), pp. 112-121. New York: Academic Press.

Emery, I. F., Bedian, V. and Guild, G. M. (1994). Differential expression of *Broad-Complex* transcription factors may forecast distinct developmental tissue fates during *Drosophila* metamorphosis. *Development* **120**, 3275-3287.

Ewer, J., Frisch, B., Hamblen-Coyle, M. J., Rosbash, M. and Hall, J. C. (1992). Expression of the *period* clock gene within different cell types in the brain of *Drosophila* adults and mosaic analysis of these cells' influence on behavioral rhythms. *J. Neurosci.* **12**, 3321-3349.

Fernandes, J. J. and Keshishian, H. (1998). Nerve-muscle interaction during flight muscle development in *Drosophila*. *Development* **125**, 1769-1779.

Fernandes, J. and VijayRaghavan, K. (1993). The development of indirect flight muscle innervation in *Drosophila melanogaster*. *Development* **118**, 215-227.

Fernandes, J., Bate, M. and VijayRaghavan, K. (1991). Development of the indirect flight muscles of *Drosophila*. *Development* **113**, 67-77.

Fernandes, J. J., Celniker, S. E. and VijayRaghavan, K. (1996). Development of the indirect flight muscle attachment sites in *Drosophila*, The role of the PS integrins and the *stripe* gene. *Dev. Biol.* **176**, 166-184.

Fristrom, D. and Fristrom, J. (1993). The metamorphic development of the adult epidermis. In *The Development of* Drosophila melanogaster (ed. M. Bate and A. Martinez-Arias), pp. 843-897. Cold Spring Harbor Laboratory Press, Cold Spring Harbor, NY.

Fristrom, D., Wilcox, M. and Fristrom, J. (1993). The distribution of PS integrins, laminin A and F-actin during key stages in *Drosophila* wing development. *Development* **117**, 509-523.

Frommer, G., Vobrüggen, G., Pasca, G., Jäckle, H. and Volk, T. (1996). Epidermal egr-like zinc-finger protein of *Drosophila* participates in myotube guidance. *EMBO J.* **15**, 1642-1649.

Gollvik, L., Kellerth, J. O. and Ulfhake, B. (1988). The effects of tenotomy and overload on the postnatal development of muscle fibre histochemistry in the cat triceps surae. *Acta Physiol. Scand.* **132**, 353-362.

Goriely, A., Dumont, N., Dambly-Chaudiere, C. and Ghysen, A. (1991). The determination of sense organs in *Drosophila*: effect of the neurogenic mutations in the embryo. *Development* **113**, 1395-1404.

Goubeaud, A., Knirr, S., Renkawitz-Pohl, R. and Paululat, A. (1996). The Drosophila gene *alien* is expressed in the muscle attachment sites during embryogenesis and encodes a protein highly conserved between plants, Drosophila and vertebrates. *Mech. Dev.* **57**, 59-68.

Halfon, M. S. and Keshishian, H. (1998). The Toll pathway is required in the epidermis for muscle development in the *Drosophila* embryo. *Dev. Biol.* **199**, 164-174.

Hartenstein, V. and Posakony, J. W. (1989). Development of adult sensilla on the wing and notum of *Drosophila melanogaster*. *Development* **107**, 389-405.

Hartenstein, V., Technau, G. M. and Campos-Ortega, J. (1985). Fate mapping in wild-type *Drosophila melanogaster*. III. A fate map of the blastoderm. *Roux's Arch. Dev. Biol.* **194**, 213-216.

Hess, N., Kronert, W. A. and Bernstein, S. I. (1989). Transcriptional and post-transcriptional regulation of *Drosophila* myosin heavy chain gene expression. In *Cellular and Molecular Biology of Muscle Development* (ed. L. Kedes and F. Stockdale), pp. 621-631. New York: Alan R. Liss.

Huang, R.-Y. and Orr, W. C. (1992). *Broad-Complex* function during oogenesis in *Drosophila melanogaster*. *Dev. Genet.* **13**, 277-288.

Huet, F., Ruiz, C. and Richards, G. (1993). Puffs and PCR: the in vivo dynamics of early gene expression during ecdysone responses in *Drosophila*. *Development* **118**, 613-627.

Hummon, M. R. and Costello, W. J. (1993). Flight muscle formation in *Drosophila* mosaics: requirement for normal *shibire* function of endocytosis. *Roux's Arch. Dev. Biol.* **202**, 95-102.

Ikeda, K. and Koenig, J. H. (1988). Morphological identification of the motor neurons innervating the dorsal longitudinal muscle of *Drosophila melanogaster*. *J. Comp. Neurol.* **273**, 436-444.

Kardon, G. (1998). Muscle and tendon morphogenesis in the avian hind limb. *Development* **125**, 4019-4032.

Karim, F. D., Guild, G. M. and Thummel, C. S. (1993). The *Drosophila Broad-Complex* plays a key role in controlling ecdysone-regulated gene expression at the onset of metamorphosis. *Development* **118**, 977-988.

Karpati, G., Carpenter, S. and Eisen, A. A. (1972). Experimental core-like lesions and nemaline rods. A correlative morphological and physiological study. *Arch. Neurol.* **27**, 237-251.

Kiss, I., Beaton, A. H., Tardiff, J., Fristrom, D. and Fristrom, J. W. (1988). Interactions and developmental effects of mutations in the *Broad-Complex* of *Drosophila melanogaster*. *Genetics* **118**, 247-259.

Kok, L. P. and Boon, M. E. (1992). *Microwave Cookbook for Microscopists*. Leiden: Coulomb Press Leyden.

Kurata, S., Saito, H. and Natori, S. (1992). The 29-kDa hemocyte proteinase dissociates fat body at metamorphosis of *Sarcophaga*. *Dev. Biol.* **153**, 115-121.

Lai-Fook, J. (1963). The structure of developing muscle insertions in insects. *J. Morphol.* **123**, 503-528.

Lawrence, P. A. (1982). Cell lineage of the thoracic muscles of *Drosophila*. *Cell* **29**, 493-503.

Lawrence, P. A. and Johnston, P. (1986). Observations on cell lineage of internal organs of *Drosophila*. *J. Embryol. Exp. Morphol.* **91**, 251-266.

Lee, J. C., VijayRaghavan, K., Celniker, S. E. and Tanouye, M. A. (1995). Identification of a *Drosophila* muscle development gene with structural homology to mammalian early growth response transcription factors. *Proc. Nat. Acad. Sci. USA* **92**, 10344-10348.

Lindsley, D. and Zimm, G. G. (1992). *The Genome of* Drosophila melanogaster. San Diego: Academic Press.

Liu, E. and Restifo, L. L. (1998). Identification of a Broad Complex-regulated enhancer in the developing visual system of *Drosophila*. *J. Neurobiol.* **34**, 253-270.

Login, G. R. and Dvorak, A. M. (1994). *The Microwave Tool Book*. Boston, MA: Beth Israel Corp.

Longhurst, C. M. and Jennings, L. K. (1998). Integrin-mediated signal transduction. *Cell. Mol. Life Sci.* **54**, 514-526.

Margolis, R. N. and Baker, J. H. (1983). Ultrastructure and biochemical changes in rat soleus muscle following tenotomy. *Anat. Rec.* **206**, 239-245.

Modolell, J. (1997). Patterning of the adult peripheral nervous system of *Drosophila*. *Perspect. Dev. Neurobiol.* **4**, 285-296.

Newman, S. M. Jr and Wright T. R. (1981). A histological and ultrastructural analysis of developmental defects produced by the mutation, *lethal(1)myospheroid*, in *Drosophila melanogaster*. *Dev. Biol.* **86**, 393-402

Pauli, D., Arrigo, A.-P. and Tissières, A. (1992). Heat shock response in *Drosophila*. *Experientia* **48**, 623-629.

Poodry, C. A. (1980). Epidermis: morphology and development. In *Genetics and Biology of* Drosophila vol. 2d (ed. M. Ashburner and T. R. F. Wright), pp. 443-497. Academic Press, New York.

Poulson, D. F. (1945). Chromosomal control of embryogenesis in *Drosophila*. *Am. Nat.* **79**, 340-363.

Prokop, A., Martín-Bermudo, M. D., Bate, M. and Brown, N. H. (1998). Absence of PS integrins or laminin A affects extracellular adhesion, but not intracellular assembly, of hemiadherens and neuromuscular junctions in *Drosophila* embyros. *Dev. Biol.* **196**, 58-76.

Prout, M., Damania, Z., Soong, J., Fristrom, D. and Fristrom, J. W. (1997). Autosomal mutations affecting adhesions between wing surfaces in *Drosophila melanogaster*. *Genetics* **146**, 275-285.

Reedy, M. C. and Beall, C. (1993a). Ultrastructure of developing flight muscles in *Drosophila*. I. Assembly of myofibrils. *Dev. Biol.* **160**, 443-465.

Reedy, M. C. and Beall, C. (1993b). Ultrastructure of developing flight muscles in *Drosophila*. II. Formation of the myotendon junction. *Dev. Biol.* **160**, 466-479.

Reedy, M. C. and Reedy, M. K. (1985). Rigor crossbridge structure in tilted single filament layers and flared-X formations from insect flight muscle. *J. Mol. Biol.* **185**, 145-176.

Restifo, L. L. and Hauglum, W. (1998). Parallel molecular genetic pathways operate during CNS metamorphosis in *Drosophila*. *Mol. Cell. Neurosci.* **11**, 134-148.

Restifo, L. L. and White, K. (1991). Mutations in a steroid hormone-regulated gene disrupt the metamorphosis of the central nervous system in *Drosophila*. *Dev. Biol.* **148**, 174-194.

Restifo, L. L. and White, K. (1992). Mutations in a steroid hormone-regulated gene disrupt the metamorphosis of internal tissues in *Drosophila*: salivary glands, muscle and gut. *Roux's Arch. Dev. Biol.* **201**, 221-234.

Reynolds, E. S. (1963). Use of lead citrate at high pH as an electron-opaque stain in electron microscopy. *J. Cell Biol.* **17**, 208-213.

Rheuben, M. B. (1992). Degenerative changes in the muscle fibers of *Manduca sexta* during metamorphosis. *J. Exp. Biol.* **167**, 91-117.

Sandstrom, D. J., Bayer, C. A., Fristrom, J. W. and Restifo, L. L. (1997). *Broad-Complex* transcription factors regulate thoracic muscle attachment in *Drosophila*. *Dev. Biol.* **181**, 168-185.

Shatoury, H. H. (1956). Developmental interactions in the development of the imaginal muscles of *Drosophila*. *J. Embryo. Exp. Morph.* **4**, 228-239.

Shilo, B.-Z. and Raz, E. (1991). Developmental control of the *Drosophila* EGF receptor homolog DER. *Trends Genet.* **7**, 388-392.

Smith, D. S. (1982). The structure of insect muscles. In *Insect Ultrastructure*, vol. 2 (ed. R. C. King and H. Akai), pp. 111-150. Plenum Press, New York.

Sokal, R. R. and Rohlf, J. F. (1993). *Biometry*. W. H. Freeman and Company, New York.

Strumpf, D. and Volk, T. (1998). Kakapo, a novel cytoskeletal-associated protein is essential for the restricted localization of the neuregulin-like factor, Vein, at the muscle-tendon junction site. *J. Cell Biol.* **143**, 1259-1270.

Tepass, U. and Hartenstein, V. (1994). The development of intercellular junctions in the *Drosophila* embryo. *Dev. Biol.* **161**, 563-596.

VijayRaghavan, K., Gendre, N. and Stocker, R. F. (1996). Transplanted wing and leg imaginal discs in *Drosophila melanogaste*r demonstrate interactions between epidermis and myoblasts in muscle formation. *Dev. Genes Evol.* **206**, 46-53.

Volk, T. and VijayRaghavan, K. (1994). A central role for epidermal segment border cells in the induction of muscle patterning in the *Drosophila* embryo. *Development* **120**, 59-70.

von Kalm, L., Crossgrove, K., Von Seggern, D., Guild, G. M. and Beckendorf, S. K. (1994). The *Broad-Complex* directly controls a tissue-specific response to the steroid hormone ecdysone at the onset of *Drosophila* metamorphosis. *EMBO J.* **13**, 3505-3516.

Vorbrüggen, G. and Jäckle, H. (1997). Epidermal muscle attachment site-specific target gene expression and interference with myotube guidance in response to ectopic *stripe* expression in the developing *Drosophila* epidermis. *Proc. Nat. Acad. Sci. USA* **94**, 8606-8611.

Williams, C. M. and Williams, M. V. (1943). The flight muscles of *Drosophila repleta*. *J. Morphol.* **72**, 589-599.

Williams, G. J. and Caveney, S. (1980). A gradient of morphogenetic information involved in muscle patterning. *J. Embryol. Exp. Morphol.* **58**, 35-61.

Yarnitzky, T., Min, L. and Volk, T. (1997). The *Drosophila* neuregulin homolog Vein mediates inductive interactions between myotubes and their epidermal attachment cells. *Genes Dev.* **11**, 2691-2700.